



Silver Nanoparticle Conjugation with Thiopyridine Exhibited Potent Antibacterial Activity Against *Escherichia coli* and Further Enhanced by Copper Capping

Ayaz Anwar^{1,2}, Samina Perveen², Shakil Ahmed², Ruqaiyyah Siddiqui¹, Muhammad Raza Shah² and Naveed Ahmed Khan^{1,*}

¹Department of Biological Sciences, School of Science and Technology, Sunway University, Bandar Sunway, Selangor, Malaysia

²H.E.J. Research Institute of Chemistry, International Center for Chemical and Biological Sciences, University of Karachi, Karachi, Pakistan

*Corresponding author: Department of Biological Sciences, School of Science and Technology, Sunway University, Selangor, 47500, Malaysia. Tel: +60-374918622, Ext: 7176, Fax: +60-356358630, Email: naveed5438@gmail.com

Received 2018 May 07; Revised 2018 August 27; Accepted 2018 August 28.

Abstract

Background: Nanomaterials-based antibacterial agents are anticipated as future generation antibiotics. Silver nanoparticles are promising candidates to enhance the antibacterial effects of antibiotic drugs and lead compounds. Pyridine compounds and thiol moieties are important classes of pharmacophores that are part of many drugs used against numerous diseases; therefore, we conjugated synthetic thiopyridine (ThPy) with silver nanoparticles.

Objectives: The study was designed to evaluate the antibacterial potential of ThPy and the effects of silver nanoparticles conjugation with it and to explore the synergistic effects of other metal ions.

Methods: Using formyl pyridine reaction with dibromopropane, N-alkylated product was obtained. Bromo group was substituted by thioacetate nucleophile resulting in the formation of thiopyridine (ThPy). Thiopyridine was used to stabilize silver nanoparticles synthesized by one-phase reduction. Silver nanoparticle-conjugated thiopyridine (ThPy-AgNPs) showed typical surface plasmon resonance band, while atomic force microscopy (AFM) showed size and morphology of spherical polydispersed nanoconjugates of 60 nm.

Results: Antibacterial properties of synthesized cationic compound thiopyridine was enhanced by conjugation with silver nanoparticles. Moreover, we presented a new strategy in which thiopyridine-AgNP nanoconjugates' affinity towards copper ions is utilized to further enhance antibacterial activity of nanoconjugates. ThPy-AgNPs exhibited more inhibitory effects against *Escherichia coli* (MIC of 100 µg/mL compared to 200 µg/mL with ThPy). Nanoconjugates showed selective affinity for Cu(I) ions to cross the *E. coli* membrane.

Conclusions: The addition of Cu(I) ions with ThPy-AgNPs has a synergistic effect on the activity of nanoconjugates against *E. coli*. Atomic force microscopy is proved to be an excellent choice to study the morphological changes occurring during the antibacterial process.

Keywords: Thiopyridine, Silver Nanoparticles, Antibacterial Activity, Synergistic Effects, *Escherichia coli*, Atomic Force Microscopy

1. Background

Nanotechnology has great potential in the treatment of bacterial infections. Metal nanoparticles can enhance the effects of marketed drugs and/or target bacteria as an alternative to antibiotics (1). For example, nanoparticles have been used as antibacterial coatings to prevent infections (2). Drugs conjugated with nanoparticles are considered as efficient drug delivery systems that suffer from poor bioavailability for enhanced activity to treat infections, while some nanoparticles have also been used for bacterial detection (2).

Silver in particular is found extraordinarily effective against several microbes (3). Its strong antimicrobial properties, chemical inertness and high thermal stability offer potential applications (3). Although silver ions possess strong antimicrobial properties, they are easily sequestered by chloride, phosphate and proteins. Silver nanoparticles are less susceptible to being intercepted and offer an effective delivery mechanism. Hence, the nanoparticle form is used preferably to ferry silver ions to bacteria for effective killing. To this end, several lines of evidence suggest that silver nanoparticles (AgNPs) exhibit potent

antibacterial properties against *Escherichia coli* by release of silver ions (4).

Several derivatives of thiopyridine are promising candidates for killing growing and dormant bacterial cells (5, 6). In bacteria, transition metals such as copper, along with iron and manganese are used as a catalyzer for electron transfer reactions in metallo-enzymes such as cytochrome oxidase (7). Copper is a vital cofactor of various enzymes, albeit free copper is highly toxic to living cells. Bacteria have developed specific copper homeostasis systems that commonly act as defense mechanisms to maintain the cellular metabolism at ambient copper concentrations (8). In Gram-negative bacteria, the inner membrane pumps heavy metal (P1B-type ATPases) transferring cytoplasmic copper to periplasm. Hence, transition metal homeostasis and detoxification are crucial factors for cell viability (9). Recently, metal ions such as Cu(II) and Hg(II) are shown to exert synergistic effects on the antibacterial activity of Ag-NPs (10, 11).

2. Objectives

Since copper species are known to affect the permeability of the outer membrane of *E. coli* (12), the overall aim of this study was to determine whether conjugation with AgNPs enhances antibacterial effects of thiopyridine. We further determined whether Cu(I) enhanced antibacterial activity of thiopyridine-conjugated silver nanoparticles against *E. coli*.

3. Methods

3.1. Chemical and Reagents

All chemicals and reagents were purchased from Sigma-Aldrich, unless otherwise stated. *Escherichia coli* was obtained from the American type culture collection (ATCC 8739). Deionized water was used for the synthesis and analysis of ThPy-AgNPs. UV-visible spectra were recorded at thermo scientific evolution 300 spectrophotometer and atomic force microscopy (AFM) analysis was carried out by the ACAFM mode on Agilent technologies 5500 AFM instrument.

3.2. Synthesis of ThPy-AgNPs

Thiopyridine and ThPy-AgNPs were synthesized as described previously (13). Briefly, 0.9 mL 4-formylpyridine (1 mmol) was stirred in 3 mL dibromopropane as a solvent. The solution was magnetically stirred and heated at 60°C for 8 hours. The brown precipitates formed after 8 hours were filtered to remove excess solvent. The precipitates were washed by chloroform to remove unreacted

formyl pyridine, followed by washing with methanol to obtain pure N-alkylated product in the viscous gummy liquid form resulting from evaporation of methanol. Next, 229 mg of N-alkylated product (1 mmol) was dissolved in 8 mL of ethanol, and 137 mg potassium thioacetate (1.2 mmol) was added to the stirring solution at room temperature.

The progress of the reaction was monitored using thin layer chromatography (dichloromethane: Methanol, 9:1). After completion of reaction (around 10 hours), ethanol was evaporated at reduced pressure to obtain a brown solid crude product. The crude product was subsequently washed with chloroform followed by methanol. 1-(3-(Acetylthio) propyl)-4-formylpyridin-1-ium (thiopyridine) was obtained from the methanol washing in brown crystalline state after slow evaporation of the solvent. Thiopyridine was characterized by Fourier transformation infrared spectroscopy, electrospray mass spectrometry and proton nuclear magnetic resonance spectroscopy.

ThPy-AgNPs (1 mM) were prepared as follows; 10:1 (v/v) thiopyridine to AgNO₃ aqueous solution was mixed and stirred for 2 hours in the presence of sodium borohydride. The reaction mixture turned yellow-brown from colorless, and the UV-visible spectral profile and AFM analysis were carried out to determine the successful formation of ThPy-coated AgNPs (13).

3.3. Minimum Inhibitory Concentration (MIC)

Agar well diffusion method was employed to calculate MICs. Briefly, MIC was measured for ThPy alone and AgNPs-coated ThPy. Briefly, Mueller Hinton agar was used as medium to develop a lawn of *E. coli* ATCC 8739 at 10⁶ cells/mL concentration. In some experiments, Mueller Hinton agar containing Cu(I) was prepared. Plates were incubated with ThPy-AgNPs and ThPy alone. Duplicate dilutions were used to calculate minimum zones of inhibition. In each well, various concentrations of ThPy-AgNPs ranging from 5 to 500 µg/mL were added. Plates were incubated for 2 hours at room temperature to facilitate the diffusion process before incubation for 24 - 48 hours at 37°C. The zones of inhibition were measured by using a millimeter scale.

3.4. Cytotoxic Activity of Cu(I) Against *Escherichia coli*

Freshly harvested *E. coli* ATCC 8739 cells isolated from tryptone soya agar were seeded at 10⁶ cells in each well of 96-well plate. Next, various concentrations of Cu(I) were serially diluted in Muller Hinton broth, then 200 µL of each concentration was added to duplicate wells and the plate was incubated for 18 - 24 hours at 37°C. Following this incubation, 20 µL of MTT (stock concentration of 5 mg/mL) was added to each well and the plate was incubated at 37°C

for 3 hours. Absorbance was recorded at 570 nm with the reference wavelength of 650 nm (14).

3.5. Inductively Coupled Plasma (ICP-OES) Spectroscopy

To examine the permeability of nanoparticles loaded with Cu(I), different doses of ThPy-AgNPs and copper (I) were incubated with *E. coli* (10^6 CFU/mL) at 37°C for 24 hours in two sets. After incubation, bacterial colonies were enumerated by plating on nutrient agar plates for one set. For the second set, bacteria were centrifuged at $12000 \times g$ for 1 hour at 4°C. The supernatants were discarded while the resultant pellet was incubated with 10 mL of 1% nitric acid for the digestion of the samples. The digested suspension was filtered using a 0.45- μ m syringe filter and analyzed by ICP-OES with standards of silver and copper, and untreated *E. coli* were used as controls (15).

3.6. Atomic Force Microscopy Imaging

Escherichia coli ATCC 8739 was cultured on tryptic soy agar (Oxoid, UK) at 37°C for 24 hours. Ten μ L of each test sample was applied onto a poly-L-lysine (PLL)-coated glass slide and allowed to dry at room temperature. Meanwhile, freshly incubated culture was diluted to make 10^6 CFU of *E. coli* in distilled water, and 10 μ L of this solution was casted onto a freshly cleaved mica surface and dried at room temperature. Next, the samples were rinsed with Milli-Q water and air-dried at room temperature. The samples were then subjected to AFM for morphological analysis. High frequency 125 μ m length Si cantilever was used with force constant of 42 N/m and resonance frequency of 330 kHz.

4. Results

Formyl pyridine reaction with dibromopropane was controlled to obtain monosubstituted product by using excessive dibromopropane (as solvent, instead of stoichiometric ratio). The obtained salt N-alkylated product was found to be an ionic liquid after removal of solvents. In the next step, bromo group was substituted by thioacetate nucleophile in polar protic solvent (Figure 1A). The optimized reaction conditions suited the formation of thiopyridine favorably as implied by high-yield and purity. Thiopyridine was finally used to stabilize silver nanoparticles synthesized by one phase reduction by sodium borohydride (13). Figure 1B describes the typical surface plasmon resonance band of the AgNPs for ThPy-conjugated AgNPs with absorption maxima at 402 nm, while 1C shows the size and morphology of spherical polydispersed nanoconjugates with the average diameter of 60 nm.

To evaluate the antibacterial effects of silver nanoparticles conjugation with thiopyridine against *E. coli*, inhibition zone assay was performed. Since ThPy-AgNPs were

found to display specific affinity towards Cu(I) ions and copper homeostasis plays a pivotal role in the defense mechanism of *E. coli*, we aimed to test the effects of intracellular interactions of Cu(I) and ThPy-AgNPs on their antibacterial potency. Bacteria were treated with multiple doses of ThPy-AgNPs, which upon conjugating with Cu(I) ions damaged the cellular walls and disrupted the morphology of the microbe (Table 1 and Figure 3). The safe Cu(I) accumulation dosage for *E. coli* ATCC 8739 is found to be less than 40 μ g/mL in which the cells can digest the Cu(I) to regulate the metabolic system. The MICs were calculated for thiopyridine and ThPy-AgNPs with and without Cu(I) ions by using the inhibition zone method as mentioned in the Methods section. Minimum inhibitory concentration of thiopyridine is calculated to be 200 μ g/mL, whereas for ThPy-AgNPs it is obtained at 100 μ g/mL.

Inductively coupled plasma (ICP) spectroscopy analysis (Table 2) showed that *E. coli* contained 0.167 ppm Cu(I) in blank samples, which strengthens our hypothesis that copper is used in the metabolism of bacteria. Different Cu(I) amounts were incubated with *E. coli*, and it can be clearly observed that at 30 to 40 ppm of test samples, the amount entering the cells of the sample increased suggesting the effective interaction of ThPy-AgNPs and Cu(I). However, at concentrations higher than 40 ppm of Cu(I), it was toxic and started to kill the bacteria. Therefore, the number of nanoparticles entering the cells declined, which further dropped down to only 1.582 ppm at 100 ppm test nanoparticles. While at 100 ppm in the absence of Cu(I), only 0.009 ppm nanoparticles were infused in the cells.

Atomic force microscopy images of control *E. coli* showed a smooth cell surface with no ruptures or indentations as displayed in Figure 2A. Figure 2B depicts the image of *E. coli* treated with 30 μ g/mL (below the MIC) Cu(I), and it is clearly evident that Cu(I)-treated cells are healthier and contain smoother surface as compared to control cells. This is due to the fact that at non-cytotoxic dosage of Cu(I) ions, these ions are used in the metabolism of *E. coli*.

Escherichia coli cultures were also treated with thiopyridine alone (MIC, 200 μ g/mL), and cell morphology was examined via AFM with variable incubation times. The images revealed a roughness in the surface after 4 hours (Figure 2C - E), while the cellular degradation increased with time, and after 8 hours, the cells were degraded. Since the unconjugated AgNPs demonstrated poor antibacterial efficiency as reported in our previous study (16), their role as cytotoxic agents against *E. coli* was ruled out. Furthermore, to balance the effect of Cu(I)-mediated infusion of nanoparticles in *E. coli*, we incubated Cu(I)-pretreated cells with thiopyridine, which showed no difference in cell morphology as compared to ligand used alone. Hence, AFM analysis was found to be in complete agreement with the

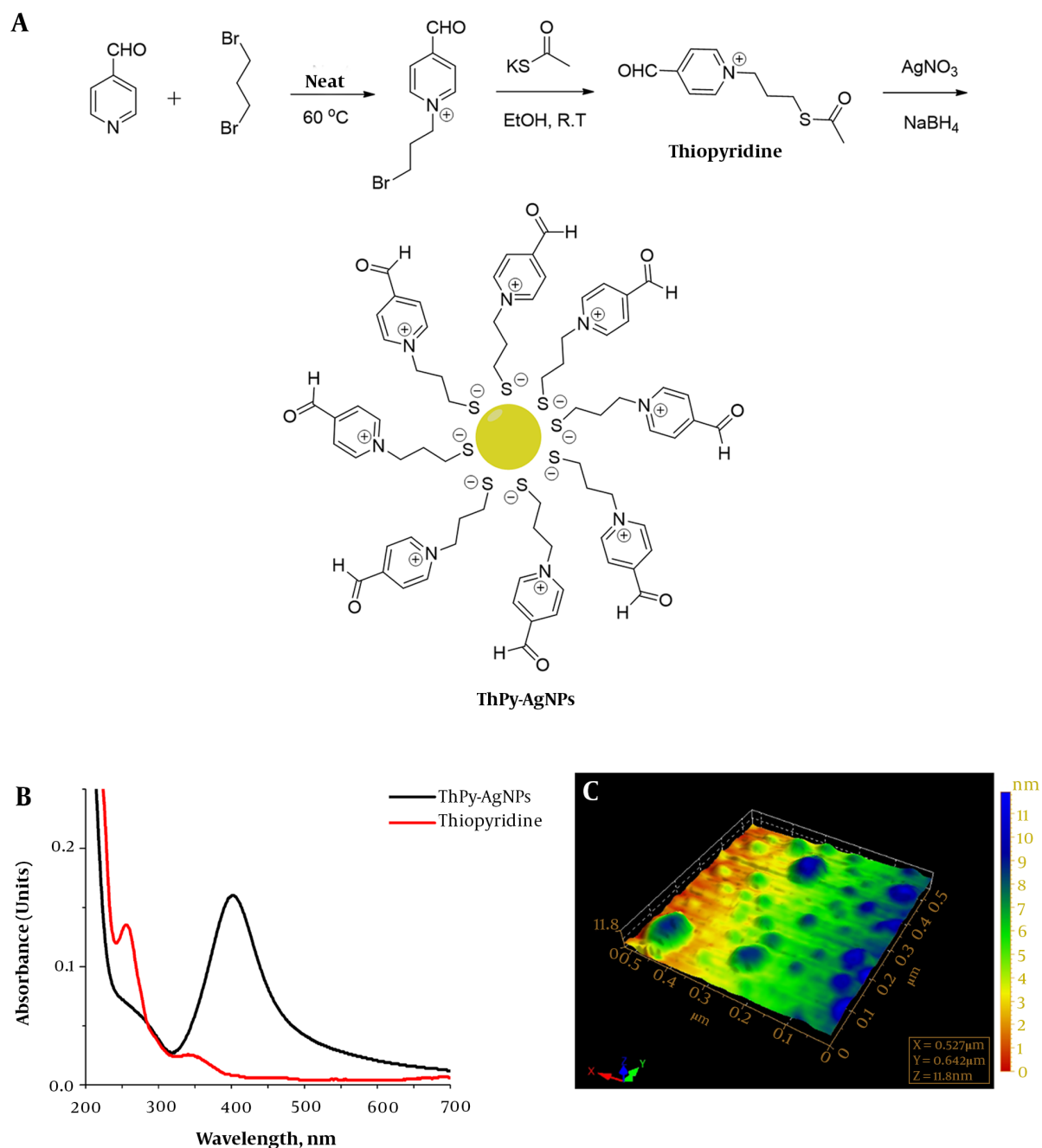


Figure 1. (A) Synthesis of thiopyridine ligand and ThPy-AgNPs, (B) UV-visible spectral profile of ThPy-AgNPs, and (C) atomic force microscopy topographic image of stabilized ThPy-AgNPs. The results are representative of three independent experiments.

MIC data. ThPy-AgNPs were found to destroy *E. coli* more effectively (MIC, 100 $\mu\text{g/mL}$) compared to thiopyridine alone (MIC, 200 $\mu\text{g/mL}$) within 4 hours (Figure 3).

5. Discussion

Here, we synthesized, characterized, and tested thiopyridine ligand and ThPy-AgNPs against *E. coli* ATCC 8739. MICs were calculated by the zone of inhibition method,

Table 1. Comparison of Concentration of Thiopyridine (ThPy) and ThPy-AgNPs with and Without Cu(I) Accumulation

Concentration, $\mu\text{g/mL}$	Zones of Inhibition, ThPy Alone, mm	Zones of Inhibition, ThPy Alone, with Cu(I), mm	Zones of Inhibition, ThPy-AgNPs, mm
5	-	-	-
10	-	-	-
25	-	-	-
50	10 ± 0.1	10.1 ± 0.3	12 ± 0.2
100	12 ± 0.2	12.3 ± 0.2	15 ± 0.2
200	15 ± 0.3	15.2 ± 0.2	17 ± 0.3
300	19 ± 0.2	19.2 ± 0.3	20 ± 0.4
400	21 ± 0.4	21.1 ± 0.3	23 ± 0.5
500	23 ± 0.3	23 ± 0.2	26 ± 0.3

Table 2. Inductively Coupled Plasma Results of Cu(I) Accumulation and ThPy-AgNPs Permeability in the Presence of Cu(I)

Tests Concentration	Copper Concentration by ICP, ppm	Silver Concentration by ICP, ppm
Blank	0.169	0.0
Blank	0.166	0.0
1	0.614	0.628
5	2.021	1.690
10	2.215	1.973
30	2.975	2.053
40	5.364	4.631
80	5.364	4.474 with 40 ppm Cu(I)
100	-	1.582 with 40 ppm Cu(I)
100	-	0.009 without Cu(I)

while AFM provided the detailed morphological events occurred at the cellular level. The membrane of *E. coli* is made up of inhomogeneous packing of lipopolysaccharide (LPS); therefore, it is a bit rough at nanoscale (17). The packing of the adjacent LPS patches is quite tight, which produces a permeable barrier (17, 18). Since metal ions play a key role in safeguarding the assembly of the LPS and membrane proteins within the outer membrane (19), these can be exploited to increase cell permeability. The use of metal ions to attain the liberation of the periplasmic substances has been presented in several literature reports (20).

Since the mode of action of nanoparticles depends on their physicochemical properties, particularly their surface features, it was observed that ThPy-AgNPs can easily penetrate the bacterial cells when pre-treated with Cu(I) by adhering to proteins in the cell membrane due to selective supramolecular interaction of ThPy-AgNPs with Cu(I) ions. On the other hand, unconjugated AgNPs and thiopyridine were found to be less effective in disrupting the cell membrane as shown in Table 1. Reports on the mechanism of antimicrobial actions of silver ions suggest that upon sil-

ver ions treatment, DNA regulation and expression of ribosomal subunit proteins alter while some other cellular proteins and enzymes producing ATP are inactivated (4). It has also been suggested that silver ions primarily disturb the function of membrane-bound enzymes, for example as in the respiratory chain (3, 4).

For thiopyridine and ThPy-AgNPs, AFM images were acquired from MIC samples and only relatively intact cells were observed. Therefore, these images represent only those cells which showed minimal cell lysis at a particular sample concentration. A logical trend is observed in the roughness of cell membrane, which increased with enhanced sample concentration, and ThPy-AgNPs had the most drastic effect on the surface roughness as suggested by the MIC data.

5.1. Conclusions

In sum, we demonstrated antibacterial action of a novel thiopyridine ligand in comparison with AgNPs after capping with it. The antibacterial activity of Cu(I)-doped

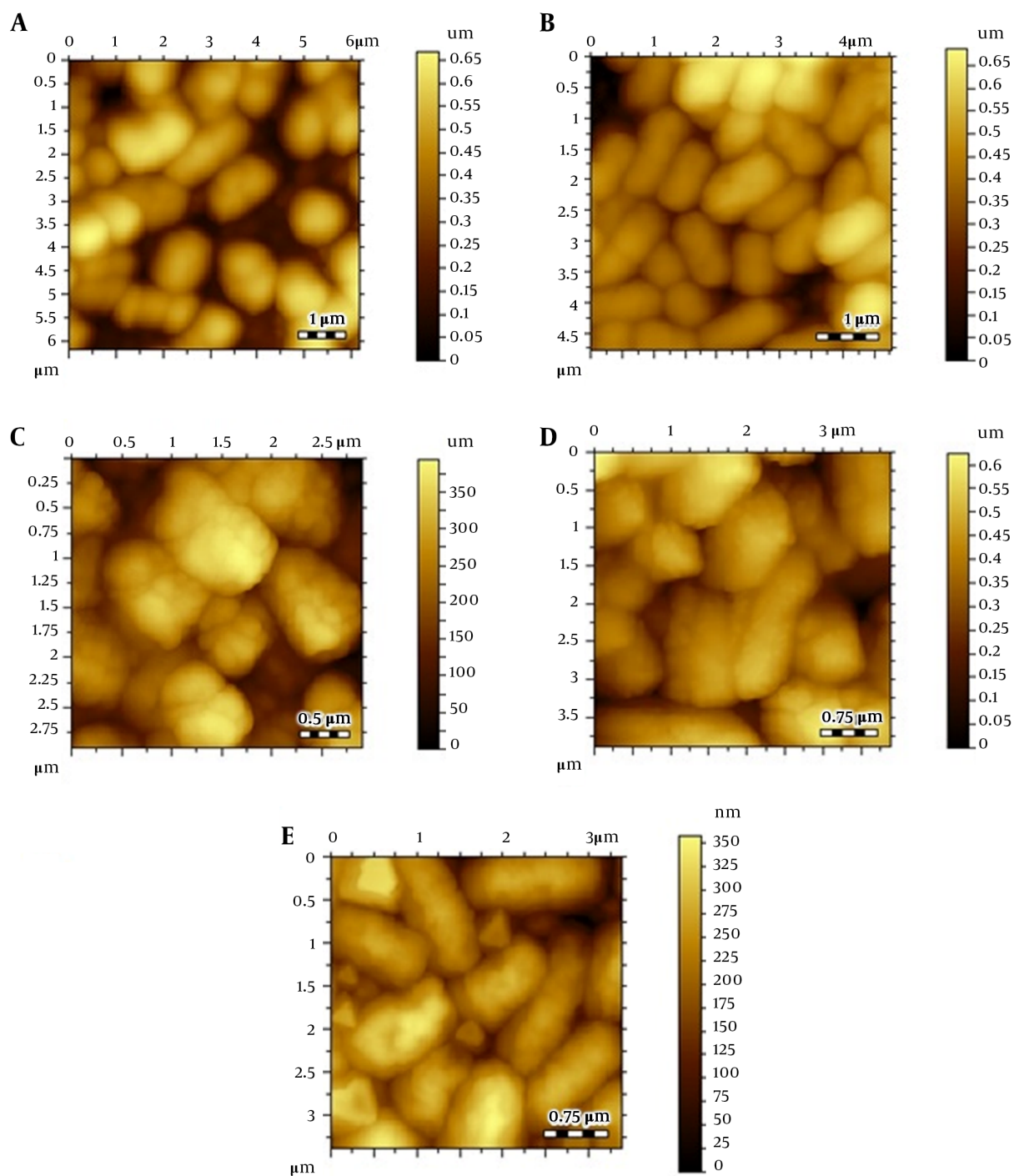


Figure 2. Atomic force microscopic images; (A) *Escherichia coli* control, (B) *E. coli* after treating Cu(I), (C) thiopyridine-treated *E. coli* at 4 hours, (D) thiopyridine-treated *E. coli* at 8 hours, and (E) thiopyridine-treated *E. coli* pretreated with Cu(I) at 4 hours. The results are representative of at least three independent experiments.

ThPy-AgNPs was studied against *E. coli* ATCC 8739. The quantitative measurements by conventional antibacterial as-

says, the use of AFM to determine surface integrity, and morphological alterations indicated that ThPy-AgNPs were

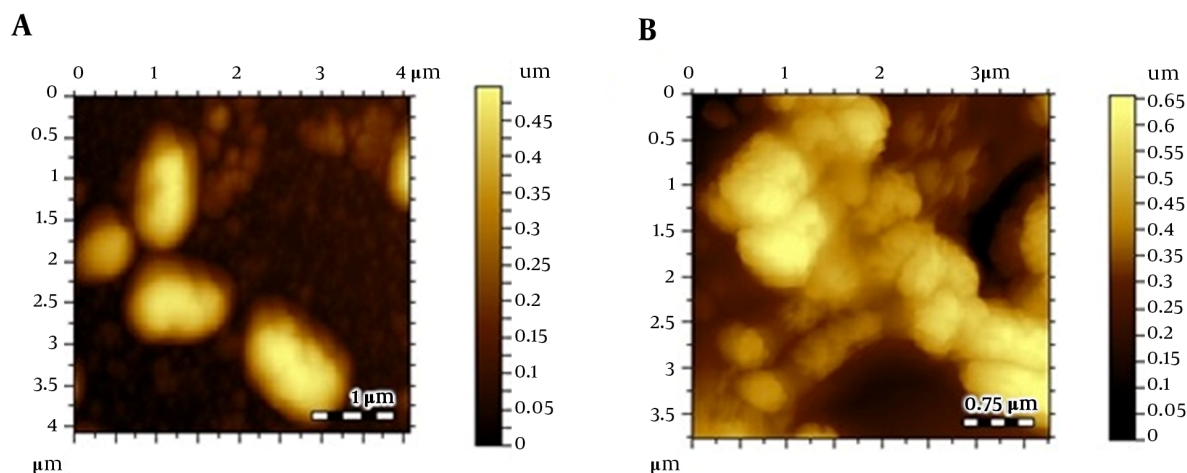


Figure 3. Atomic force microscopic images; ThPy-AgNPs-treated *Escherichia coli* pretreated with Cu(I) at (A) 4 hours (B) 8 hours. The results are representative of at least three independent experiments

twice as effective as free thiopyridine ligand in *E. coli* lysis. The lower concentration of Cu(I) maximized cell permeability of ThPy-AgNPs without exhibiting cytotoxicity. This work clearly demonstrates that integrating nanotechnology and microbiology can lead to possible advancement in the formulation of new types of antibacterial agents.

Acknowledgments

Authors acknowledge Higher Education Commission (HEC) of Pakistan and Sunway University for financial support.

Footnotes

Authors' Contribution: Ayaz Anwar and Samina Perveen synthesized and characterized the materials under the supervision of Muhammad Raza Shah. Ayaz Anwar and Shakil Ahmed planned and performed the antibacterial experiments. Ayaz Anwar and Ruqaiyyah Siddiqui analyzed the data under the supervision of Naveed Ahmed Khan. Ayaz Anwar and Naveed Ahmed Khan wrote the manuscript. All the authors approved the manuscript.

Conflict of Interests: No conflict of interest exists.

Ethical Considerations: This article does not contain any studies with human participants or animals performed by authors.

Financial Disclosure: None declared.

Funding/Support: Authors are thankful of Higher Education Commission (HEC) of Pakistan and Sunway University for funding.

References

- Hajipour MJ, Fromm KM, Ashkarran AA, Jimenez de Aberasturi D, de Larramendi IR, Rojo T, et al. Antibacterial properties of nanoparticles. *Trends Biotechnol.* 2012;**30**(10):499-511. doi: [10.1016/j.tibtech.2012.06.004](https://doi.org/10.1016/j.tibtech.2012.06.004). [PubMed: 22884769].
- Chen X, Jiang B, Hamza T, Li B. Nanoparticles targeting to osteoblasts for potential intracellular pathogen elimination. *J Control Release.* 2015;**213**:e10-1. doi: [10.1016/j.jconrel.2015.05.013](https://doi.org/10.1016/j.jconrel.2015.05.013). [PubMed: 27005022].
- Morones JR, Elechiguerra JL, Camacho A, Holt K, Kouri JB, Ramirez JT, et al. The bactericidal effect of silver nanoparticles. *Nanotechnol. 2005*;16(10):2346-53. doi: [10.1088/0957-4484/16/10/059](https://doi.org/10.1088/0957-4484/16/10/059). [PubMed: 20818017].
- Pal S, Tak YK, Song JM. Does the antibacterial activity of silver nanoparticles depend on the shape of the nanoparticle? A study of the Gram-negative bacterium *Escherichia coli*. *Appl Environ Microbiol.* 2007;**73**(6):1712-20. doi: [10.1128/AEM.02218-06](https://doi.org/10.1128/AEM.02218-06). [PubMed: 17261510]. [PubMed Central: PMC1828795].
- Klimesova V, Svoboda M, Waisser K, Pour M, Kaustova J. New pyridine derivatives as potential antimicrobial agents. *Farmaco.* 1999;**54**(10):666-72. doi: [10.1016/S0014-827X\(99\)00078-6](https://doi.org/10.1016/S0014-827X(99)00078-6). [PubMed: 10575735].
- Patel NB, Agravat SN, Shaikh FM. Synthesis and antimicrobial activity of new pyridine derivatives-I. *Med Chem Res.* 2010;**20**(7):1033-41. doi: [10.1007/s00044-010-9440-0](https://doi.org/10.1007/s00044-010-9440-0).
- Porcheron G, Garenaux A, Proulx J, Sabri M, Dozois CM. Iron, copper, zinc, and manganese transport and regulation in pathogenic Enterobacteria: Correlations between strains, site of infection and the relative importance of the different metal transport systems for virulence. *Front Cell Infect Microbiol.* 2013;**3**:90. doi: [10.3389/fcimb.2013.00090](https://doi.org/10.3389/fcimb.2013.00090). [PubMed: 24367764]. [PubMed Central: PMC3852070].
- Rademacher C, Masepohl B. Copper-responsive gene regulation in bacteria. *Microbiology.* 2012;**158**(Pt 10):2451-64. doi: [10.1099/mic.0.058487-0](https://doi.org/10.1099/mic.0.058487-0). [PubMed: 22918892].
- Gourdon P, Liu XY, Skjorringe T, Morth JP, Moller LB, Pedersen BP, et al. Crystal structure of a copper-transporting PIB-type ATPase. *Nature.* 2011;**475**(7354):59-64. doi: [10.1038/nature10191](https://doi.org/10.1038/nature10191). [PubMed: 21716286].

10. Rasheed W, Perveen S, Mustafa G, Shah MR, Ahmed S, Uzzaman S. Impact of Cu(II)-doping on the vulnerability of Escherichia coli ATCC 10536 revealed by Atomic Force Microscopy. *Micron*. 2018;**110**:73–8. doi: [10.1016/j.micron.2018.05.002](https://doi.org/10.1016/j.micron.2018.05.002). [PubMed: [29772475](https://pubmed.ncbi.nlm.nih.gov/29772475/)].
11. Rasheed W, Shah MR, Perveen S, Ahmed S, Uzzaman S. Revelation of susceptibility differences due to Hg(II) accumulation in Streptococcus pyogenes against CX-AgNPs and Cefixime by atomic force microscopy. *Ecotoxicol Environ Saf*. 2018;**147**:9–16. doi: [10.1016/j.ecoenv.2017.08.030](https://doi.org/10.1016/j.ecoenv.2017.08.030). [PubMed: [28822261](https://pubmed.ncbi.nlm.nih.gov/28822261/)].
12. Mermod M, Magnani D, Solioz M, Stoyanov JV. The copper-inducible ComR (YcfQ) repressor regulates expression of ComC (YcfR), which affects copper permeability of the outer membrane of Escherichia coli. *Biometals*. 2012;**25**(1):33–43. doi: [10.1007/s10534-011-9510-x](https://doi.org/10.1007/s10534-011-9510-x). [PubMed: [22089859](https://pubmed.ncbi.nlm.nih.gov/22089859/)].
13. Anwar A, Shah MR, Pir Muhammad S, Afridi S, Ali K. Thio-pyridinium capped silver nanoparticle based supramolecular recognition of Cu(i) in real samples and T-lymphocytes. *New J Chem*. 2016;**40**(7):6480–6. doi: [10.1039/c5nj03609g](https://doi.org/10.1039/c5nj03609g).
14. Piaru SP, Perumal S, Cai LW, Mahmud R, Majid AMSA, Ismail S, et al. Chemical composition, anti-angiogenic and cytotoxicity activities of the essential oils of Cymbopogon citratus (lemon grass) against colorectal and breast carcinoma cell lines. *J Essent Oil Res*. 2012;**24**(5):453–9. doi: [10.1080/10412905.2012.703496](https://doi.org/10.1080/10412905.2012.703496).
15. Li F, Zhao Q, Wang C, Lu X, Li XF, Le XC. Detection of Escherichia coli O157:H7 using gold nanoparticle labeling and inductively coupled plasma mass spectrometry. *Anal Chem*. 2010;**82**(8):3399–403. doi: [10.1021/ac100325f](https://doi.org/10.1021/ac100325f). [PubMed: [20307076](https://pubmed.ncbi.nlm.nih.gov/20307076/)].
16. Shah MR, Ali S, Ateeq M, Perveen S, Ahmed S, Bertino MF, et al. Morphological analysis of the antimicrobial action of silver and gold nanoparticles stabilized with ceftriaxone on Escherichia coli using atomic force microscopy. *New J Chem*. 2014;**38**(11):5633–40. doi: [10.1039/c4nj00751d](https://doi.org/10.1039/c4nj00751d).
17. Croxen MA, Finlay BB. Molecular mechanisms of Escherichia coli pathogenicity. *Nat Rev Microbiol*. 2010;**8**(1):26–38. doi: [10.1038/nrmicro2265](https://doi.org/10.1038/nrmicro2265). [PubMed: [19966814](https://pubmed.ncbi.nlm.nih.gov/19966814/)].
18. Coughlin RT, Caldwell CR, Haug A, McGroarty EJ. A cationic electron spin resonance probe used to analyze cation interactions with lipopolysaccharide. *Biochem Biophys Res Commun*. 1981;**100**(3):1137–42. doi: [10.1016/0006-291X\(81\)91942-2](https://doi.org/10.1016/0006-291X(81)91942-2). [PubMed: [6268080](https://pubmed.ncbi.nlm.nih.gov/6268080/)].
19. Coughlin RT, Tonsager S, McGroarty EJ. Quantitation of metal cations bound to membranes and extracted lipopolysaccharide of Escherichia coli. *Biochemistry*. 1983;**22**(8):2002–7. doi: [10.1021/bi00277a041](https://doi.org/10.1021/bi00277a041). [PubMed: [6342672](https://pubmed.ncbi.nlm.nih.gov/6342672/)].
20. Amro NA, Kotra LP, Wadu-Mesthrige K, Bulychev A, Mobashery S, Liu GY. High-resolution atomic force microscopy studies of the Escherichia coli outer membrane: Structural basis for permeability. *Langmuir*. 2000;**16**(6):2789–96. doi: [10.1021/la991013x](https://doi.org/10.1021/la991013x).